Research Paper

A single-cysteine mutant and chimeras of essential *Leishmania* Erv can complement the loss of Erv1 but not of Mia40 in yeast

Sandra Specht[a], Linda Liedgens[a], Margarida Duarte[b,c], Alexandra Stiegler[d], Ulrike Wirth[d], Maike Eberhardt[a], Ana Tomás[b,c,e], Kai Hell[d,1,*], Marcel Deponte[a,f,1,**]

[a] Department of Parasitology, Ruprecht-Karls University, D-69120 Heidelberg, Germany
[b] i3S - Instituto de Investigação e Inovação em Saúde, Universidade do Porto, Porto 4200, Portugal
[c] Institute for Molecular and Cell Biology - IBMC, Universidade do Porto, 4200-135 Porto, Portugal
[d] Biomedical Center Munich - Physiological Chemistry, Ludwig-Maximilians University, D-82152 Planegg, Martinsried, Germany
[e] ICBAS - Instituto de Ciências Biomédicas Abel Salazar, Universidade do Porto, Porto 4050-313, Portugal
[f] Faculty of Chemistry - Biochemistry, Kaiserslautern University, D-67663 Kaiserslautern, Germany

ARTICLE INFO

ABSTRACT

Mia40/CHCHD4 and Erv1/ALR are essential for oxidative protein folding in the mitochondrial intermembrane space of yeast and mammals. In contrast, many protists, including important apicomplexan and kinetoplastid parasites, lack Mia40. Furthermore, the Erv homolog of the model parasite *Leishmania tarentolae* (*Lt*Erv) was shown to be incompatible with *Saccharomyces cerevisiae* Mia40 (*Sc*Mia40). Here we addressed structure-function relationships of *Sc*Erv1 and *Lt*Erv as well as their compatibility with the oxidative protein folding system in yeast using chimeric, truncated, and mutant Erv constructs. Chimeras between the N-terminal arm of *Sc*Erv1 and a variety of truncated *Lt*Erv constructs were able to rescue yeast cells that lack *Sc*Erv1. Yeast cells were also viable when only a single cysteine residue was replaced in *Lt*Erv^{C17S}. Thus, the presence and position of the C-terminal arm and the kinetoplastida-specific second (KISS) domain of *Lt*Erv did not interfere with its functionality in the yeast system, whereas a relatively conserved cysteine residue before the flavodomain rendered *Lt*Erv incompatible with *Sc*Mia40. The question whether parasite Erv homologs might also exert the function of Mia40 was addressed in another set of complementation assays. However, neither the KISS domain nor other truncated or mutant *Lt*Erv constructs were able to rescue yeast cells that lack *Sc*Mia40. The general relevance of Erv and its candidate substrate small Tim1 was analyzed for the related parasite *L. infantum*. Repeated unsuccessful knockout attempts suggest that both genes are essential in this human pathogen and underline the potential of mitochondrial protein import pathways for future intervention strategies.

1. Introduction

The vast majority of mitochondrial proteins are synthesized at cytosolic ribosomes and have to be imported into one of the four mitochondrial compartments [1]. One of these compartments, the intermembrane space (IMS) between the inner and outer mitochondrial membrane, harbors proteins that contribute to respiration, programmed cell death, the assembly of protein complexes, and the transfer of ions, metabolites and proteins [2–6]. In addition to a functional classification, IMS proteins can be also grouped according to their protein import pathway (reviewed in [2,7]): One group of

proteins, hereinafter referred to as class I proteins, contains a positively charged N-terminal matrix-targeting signal that is followed by a hydrophobic transmembrane segment. This bipartite pre-sequence is recognized by the TIM23 complex, which inserts class I proteins into the inner mitochondrial membrane where they often undergo limited proteolysis. For example, yeast cytochrome b_2 is imported via this pathway and its soluble domain is subsequently released into the IMS by the inner membrane protease Imp1 [8–10]. Another group of proteins from yeast and mammals, hereinafter referred to as class 2 proteins, is oxidatively trapped in the IMS by a system that consists of Mia40 and Erv1 in yeast or the respective mammalian homologs CHCHD4 and ALR

[2,11–17]. The oxidoreductase Mia40 recognizes substrates with twin Cx$_3$C- or twin Cx$_9$C-motifs as well as proteins with more specialized cysteine patterns such as Erv1 [3,7,17–20]. Reference substrates of this pathway in *Saccharomyces cerevisiae* include the twin Cx$_3$C proteins *Sc*Tim9 and *Sc*Tim13, the twin Cx$_9$C cytochrome c oxidase assembly factor *Sc*Pet191, and the copper chaperone for superoxide dismutase *Sc*Ccs1 [11,12,15,21–24]. During protein import, the reduced substrates undergo one or two rounds of dithiol-disulfide exchange reactions with the oxidized CPC-motif of Mia40, yielding the trapped oxidized substrate and reduced Mia40 [13,25–31]. Reduced Mia40 is subsequently oxidized by the flavoprotein Erv1, which transfers the electrons to cytochrome *c* and the respiratory chain [25,30,32–37]. In addition, *Sc*Erv1 was also suggested to transfer electrons to molecular oxygen, yielding H$_2$O$_2$ as a substrate of cytochrome c peroxidase [36], and to fumarate with the help of the fumarate reductase Osm1 [38].

As outlined above, oxidative protein folding in the IMS has been intensely studied in yeast and mammals. These organisms belong to the same group of eukaryotes termed Opisthokonta [39]. In contrast, numerous protists have no Mia40 homolog, although their genomes encode an Erv homolog as well as candidate substrates with twin Cx$_3$C- or twin Cx$_9$C-motifs [16,40–44]. This raises the fundamental question whether several of the major groups of eukaryotes have a replacement for Mia40 or whether their Erv homologs can oxidatively fold substrates without Mia40. Among the protists without a Mia40 homolog are numerous important non-related apicomplexan and kinetoplastid parasites, such as the causative agents of malaria (*Plasmodium falciparum*), sleeping sickness (*Trypanosoma brucei*), and visceral leishmaniasis (*Leishmania infantum*). Depletion of *T. brucei* Erv (*Tb*Erv) by RNA interference was shown to result in growth arrest and mitochondrial swelling [44]. Furthermore, down regulation of *Tb*Erv in combination with quantitative proteomics revealed the down regulation of 13 proteins with twin Cx$_3$C- or twin Cx$_9$C-motifs and led to the identification of 25 candidate substrates in the IMS of *T. brucei* [45]. The depletion studies strongly support a crucial role of *Tb*Erv in oxidative protein folding. However, it remains to be analyzed whether Erv is generally essential for kinetoplastid parasites and how oxidative protein folding can occur without Mia40. We previously showed that the IMS of the kinetoplastid model parasite *Leishmania tarentolae* harbors an Erv homolog (*Lt*Erv) as well as a twin Cx$_3$C protein termed small Tim 1 (*Lts*Tim1). Both proteins as well as the twin Cx$_3$C protein *Sc*Tim9 from yeast were imported into isolated mitochondria from *L. tarentolae* and yeast, suggesting that the import signals and the oxidative folding pathway have been functionally conserved during the course of evolution [42]. Heterologous *Lt*Erv was also imported into the IMS of yeast mitochondria *in vivo*. However, neither *Lt*Erv nor an Erv homolog from *P. falciparum* (*Pf*Erv) could functionally replace essential *Sc*Erv1 in yeast [43]. Here we (i) addressed the physiological relevance of Erv and small Tim1 for survival of the deadly human pathogen *L. infantum*, (ii) determined structure-function relationships of *Sc*Erv1 and *Lt*Erv, and (iii) analyzed the compatibility of *Lt*Erv with the oxidative protein folding system in yeast.

2. Materials and methods

2.1. L. infantum cell culture

L. infantum promastigotes (strain MHOM MA67ITMAP263) were cultured at 25 °C in RPMI 1640 Glutamax supplemented with 10% (v/v) inactivated fetal bovine serum (iFBS), 50 U/mL penicillin, 50 mg/mL streptomycin (Gibco), and 25 mM HEPES sodium salt, pH 7.4 (Sigma). Parasites were synchronized by three or four daily passages of 1×10^6 cells/mL and subsequently seeded at 10^6 cells/mL (day 0). Afterwards, growth curves for wild-type and mutant strains were recorded for up to 7 days by determining the cell density in a hemocytometer.

2.2. Generation of L. infantum knockout and rescue constructs

Fragments of the 5′ and 3′ UTRs of *L. infantum ERV* (*LIERV*) for homologous recombination were PCR-amplified from *L. infantum* genomic DNA using primer pairs P1/P2 and P3/P4 (Table S1). Both PCR products were cloned into the *Hin*dIII/*Spe*I and *Bam*HI/*Xba*I restriction sites of plasmids pGL345 and pGL726, which carry coding sequences for hygromycin B phosphotransferase (*HygR*) or phleomycin hydrolase (*PhleoR*), respectively. Deletion constructs for *L. infantum small TIM1* (*LIsTIM1*) were generated likewise. Fragments of the 5′ and 3′ UTRs of *LIsTIM1* were PCR-amplified with primers P5/P6 and P7/P8 (Table S1) and cloned into the *Hin*dIII/*Spe*I and *Bam*HI//*Xba*I restriction sites of pGL345 and pGL726. Before transfection of *L. infantum*, the replacement cassettes were excised from the plasmids by digestion with *Hin*dIII/*Bgl*II and purified from agarose gels. Rescue plasmid pTEX-NEO-*LIERV* was assembled by cloning the *LIERV* ORF, which was PCR-amplified with primers P9/P10 (Table S1), into the *Bam*HI/*Hin*dIII restriction sites of pTEX-NEO. This trypanosomatid expression vector carries a coding sequence for the neomycin phosphotransferase (*NeoR*) [46]. To generate the pTEX-NEO-*LIsTIM* rescue plasmid, the *LIsTIM* ORF was PCR-amplified with primer pair P11/P12 (Table S1) and cloned into the *Bam*HI/*Xho*I sites of pTEX-NEO.

2.3. L. infantum transfection and selection

Transfections were performed in an Amaxa Nucleofector (Lonza) using program U-033 as described previously [47]. Briefly, 5×10^7 logarithmic phase promastigotes were suspended in Human T Cell Nucleofector (Lonza) and transfected with 2–10 µg DNA. Parasites were allowed to recover in 10 mL of culture medium without selection drug for 24 h before centrifugation and plating on medium M199 agar plates containing 10% (v/v) iFBS, 50 U/mL penicillin, 50 mg/mL streptomycin, 0.1 mM adenine, 0.023 mM hemin, 25 mM HEPES sodium salt, pH 7.4 (all from Sigma), and the selective drug(s). Hygromycin (Invitrogen) was used at 15 µg/mL, G418 (Sigma) at 15 µg/mL, and phleomycin (Sigma) at 17.5 µg/mL. Colonies were picked after 1–2 weeks and transferred to liquid medium.

2.4. Generation and site-directed mutagenesis of yeast constructs

Full length *LTERV, LTERV*^{C17S}*, LTERV*^{C63S}*, LTERV*^{C300S} and *LTERV*$^{C300S/C304S}$ in plasmid pQE30 as well as *SCERV1* and *PFERV* in pYX232 were cloned previously [43]. Additional mutant and chimeric pYX232-*LTERV* constructs were generated as follows. *LTERV*$^{C92S/C109S}$ in pQE30 was generated by two rounds of site-directed mutagenesis using primer pairs P26/P27 and P28/P29 (Table S2) and pQE30-*LTERV* as a template. *LTERV, LTERV*^{C17S}*, LTERV*^{C63S}*, LTERV*^{C300S}*, LTERV*$^{C300S/C304S}$ and *LTERV*$^{C92S/C109S}$ were PCR-amplified using primer pair P30/P31 (Table S2) with the according pQE30 constructs as templates. The truncated constructs *LTERV*$^{C-term}$ and *LTERV*$^{N-term}$ were PCR-amplified using primer pairs P32/P31 and P30/P33 (Table S2) with pQE30-*LTERV* as a template. *Chimera 1–5* were amplified by overlap extension PCR according to a standard protocol [48] using sense primer P34, overlap primer pair P35/P36 or P37/P38, and one of the antisense primers P39-P41 (Table S2) with pYX232-*SCERV1* and pYX232-*LTERV* as templates. Fusion constructs encoding the N-terminal mitochondrial targeting signal and transmembrane segment of *Sc*Mia40 (Mia40N) *MIA40N-PFERV*, *MIA40N-LTERV*, *MIA40N-LTERV*$^{N-term}$, *MIA40N-LTERV*$^{C-term}$, *MIA40N-LTERV*^{C17S} and *MIA40N-Chimera 1–6* were also amplified by overlap extension PCR using the sense primer P48, one of the overlap primers P51-54, and one of the antisense primers P31/P33/P40/P41/P50. All PCR products were subsequently cloned into the *Eco*RI/*Xho*I restriction sites of the yeast expression vector pYX232. *Chimera 6* was generated by site-directed mutagenesis using primer pair P42/P43 (Table S2). The truncated Mia40 variant *SCMIA40*^{short} (encoding residues 1–70 and 284–403) was previously cloned into the

single-copy plasmid pRS314 [49] and was a kind gift by Johannes Herrmann. All constructs were confirmed by commercial sequencing (GATC Biotech).

2.5. Yeast cell culture and complementation assays

S. cerevisiae cells were grown at 30 °C in 1% yeast extract, 2% peptone (YP) medium or in synthetic (S) minimal medium supplemented with or without the amino acids lysine, leucine, histidine, and tryptophan as well as the bases adenine and uracil [50]. For growth analysis, the medium contained either 2% glucose (YPD, SD), 3% galactose (SGal) or 3% glycerol (SG). Plasmid shuffling experiments were performed as described previously [43] with a YPH501-derived Δ*erv1* strain (genotype *ura3-52, lys2-801*^amber, *ade2-101*^ocre, *trp1-Δ63, his3-Δ200, leu2-Δ1, erv1::His3*) that harbors a *SCERV1* copy under control of the *MET25* promotor on the *URA3*-containing plasmid pRS426 [51]. Briefly, cells were transformed with the *TRP1*-containing plasmids pYX232-*SCERV1*, pYX232-*LTERV*, pYX232-*Chimera 1–6*, pYX232-*LTERV*^C-term, pYX232-*LTERV*^N-term, pYX232-*LTERV*^C17S, pYX232-*LTERV*^C63S, pYX232-*LTERV*^C92S/C109S, pYX232-*LTERV*^C300S, pYX232-*LTERV*^C300S/C304S and the respective *MIA40N* constructs according to a standard protocol [52]. After transfection and selection on SD agar plates without histidine, uracil and tryptophan, yeast strains were grown overnight in uracil-containing liquid medium. Overnight cultures were diluted in sterile water to an optical density at 600 nm (OD600) of 0.1 and further diluted 1:10, 1:100 and 1:1000. Drops (10 μL) of the overnight cultures and each serial dilution were spotted on SD agar plates without histidine and tryptophan containing 50 mg/L uracil and 1 g/L 5-fluoroorotic acid (FOA) for negative selection and plasmid shuffling [53]. The same dilutions were spotted on SD agar plates without uracil, histidine and tryptophan as a control. Analogous complementation assays for plasmids pYX232-*PFERV*, pYX232-*LTERV*, pYX232-*LTERV*^C-term, pYX232-*LTERV*^N-term, pYX232-*LTERV*^C17S, the respective *MIA40N* constructs and pRS314-*SCMIA40*^short were performed with a Δ*mia40* strain, which has the same genetic background with a *mia40::S.pombeHis5* instead of the *erv1::His3* replacement. This strain harbors a copy of a short functional version of *SCMIA40* under the control of its endogenous promoter on the *URA3*-containing plasmid pRS316 [49]. All plates were incubated at 30 °C or the indicated temperature for up to one week. Single colonies or, in the absence of colonies, swabs of background cells from FOA plates were subsequently incubated overnight or for up to 3 days in 1 mL FOA- and uracil-containing SD liquid medium (either without histidine and tryptophan in the case of Δ*erv1* cells or without tryptophan when handling Δ*mia40* cells). If cell growth was detected, liquid cultures were diluted as described above and 10 μL drops of each dilution were spotted again on FOA- and uracil-containing SD agar plates without histidine and tryptophan as well as SD agar control plates without FOA, uracil, histidine and tryptophan in order to validate the genotype.

2.6. Cell fractionation and western blot analysis

Clones from plasmid shuffling experiments that only grew on uracil-containing medium were incubated in 50 mL SD liquid medium without histidine and tryptophan until they had reached an OD600 of 1.0–1.8. Ten OD volumes of cells were harvested by centrifugation (1750 × *g*, 10 min, 4 °C) and disrupted as described previously [54]. Briefly, yeast cells were resuspended in 300 μL ice-cold buffer containing 0.6 M sorbitol, 80 mM KCl, 20 mM MOPS, pH 7.4 that was freshly supplemented with 1 mM phenylmethylsulfonyl fluoride (PMSF) before 200 μL glass beads (∅ 0.5 mm, Sigma-Aldrich) were added. The mixture was vortexed six times for 30 s before glass beads and cell debris were removed by centrifugation (1000 × *g*, 3 min, 4 °C). The supernatant was centrifuged again (20,000 × *g*, 15 min, 4 °C) to separate the mitochondria-containing pellet fraction from the cytosol-containing supernatant fraction. The pellet fraction was directly boiled in 2 × SDS-

PAGE Laemmli-buffer. The supernatant fraction was precipitated by the addition of 5–6 volumes of ice-cold acetone to 150 μL supernatant and incubated overnight at − 20 °C. The mixture was subsequently centrifuged (15,000 × *g*, 15 min, 4 °C) and the precipitate was air dried for 15 min at room temperature before boiling in 2 × SDS-PAGE Laemmli-buffer. For western blot analysis, 20 μL of the pellet sample and 10 μL of the supernatant sample were separated by SDS-PAGE on a 15% gel followed by wet blotting and immunodecoration with antibodies against *Lt*Erv (1:500 [42]), *Sc*Erv1 (1:2000 [13]), *Sc*Zwf1 (1:10000 [55]), and *Sc*Tim50 (1:250 [56]). Samples for western blot analysis of *L. infantum* promastigotes were prepared as follows. Parasites were harvested by centrifugation (3000 × *g*, 10 min, 4 °C) and washed twice in ice-cold PBS. Parasites were suspended at 6.25×10^8 cells/mL in 4% (w/v) SDS, 50 mM Tris-HCl, pH 7.4 and stored at − 70 °C until further use. Before separation by SDS-PAGE, 8 μL extracts were mixed with 12 μL PBS and 5 μL 5 × SDS-PAGE Laemmli-buffer and heated for 10 min at 65 °C.

2.7. Yeast DNA extraction and PCR analysis

Plasmid DNA was extracted from yeast as described previously [57]. For PCR analysis, 1 μL of extracted DNA was mixed with 1 μM of primer pairs P44/P45, P44/P46, and P47/P45, 400 μM dNTP mix (Thermo Scientific) and 2.5 U *Taq* DNA polymerase (NEB) in a final volume of 50 μL to amplify *SCERV1, Chimera 3*, and *Chimera 6*, respectively. Initial denaturation was carried out at 94 °C for 2 min, followed by 30 cycles of denaturation at 94 °C for 45 s, annealing at 60 °C for 45 s, and elongation at 68 °C for 45 s. The last cycle was followed by a final elongation step at 68 °C for 90 s.

2.8. Yeast growth assays on agar plates and in liquid medium

For growth assays on agar plates, yeast strains were incubated in 1 mL liquid SD medium without histidine and tryptophan and cultured in the logarithmic growth phase for up to five days. Drop dilutions assays in sterile water were subsequently performed as described above. Dilutions were spotted on SD, SG or SGal agar plates without histidine and tryptophan. All plates were incubated at 30 °C for up to 12 days. Growth assays in liquid medium were performed in a Tecan Infinite F200 Pro plate reader using transparent flat bottom 96-well-plates (Greiner). Briefly, 200 μL of liquid cultures in SD, SG or SGal medium were diluted to an absorbance of 0.1 in the according medium and were grown at 30 °C for 48 h. Plates were shaken at 183 rpm for 550 s before each hourly measurement.

2.9. Protein import into isolated mitochondria

Radiolabeled Tim13 precursor protein was synthesized *in vitro* in a TNT-coupled reticulocyte lysate system according to the manufacturer's standard protocol (Promega). Mitochondria were isolated as described [13] and quantified based on their protein content using a Bradford protein assay (BioRad). The import of Tim13 precursor protein into isolated mitochondria was performed in import buffer [56] containing 0.1 mg/mL BSA, 5 mM NADH, 2.5 mM ATP and 2 mM 2-mercaptoethanol. The import reaction contained 15% of lysate and 100 μg of mitochondria in 100 μL import buffer. The import reaction was incubated for 10 min at 25 °C and then stopped by diluting the reaction tenfold with ice-cold SH-buffer (0.6 M sorbitol, 20 mM HEPES-KOH, pH 7.4) with 50 μg/mL proteinase K. Proteinase K treatment was performed for 20 min and then stopped by addition of 2 mM PMSF. Following isolation of mitochondria, the import of precursor protein was analyzed by SDS-PAGE and autoradiography.

2.10. Mia40 redox mobility shift assays

Mitochondria (1 mg/mL) were incubated for 20 min at 25 °C in SH-

buffer with or without 5 mM reduced glutathione (GSH). Following incubation, the samples were treated for 20 min at 25 °C with 40 mM iodoacetamide in 50 mM Tris (pH 8.0), 0.6 M sorbitol to prevent artificial oxidation. The redox state of re-isolated mitochondria was analyzed by non-reducing SDS-PAGE and western blotting with antibodies against *Sc*Mia40. The buffers used were first degassed for 10 min using a Vario vacuum pump (Vacuubrand) and then flushed with nitrogen. All sample cups were also flushed with nitrogen.

2.11. Ni-NTA pull-down of His-tagged ScMia40

Pull-down assays were performed with a yeast strain that encodes a His-tagged version of *Sc*Mia40 on the plasmid pYX142 replacing wild type *Sc*Mia40 [27]. This strain was transformed with the plasmid pYX232-*Chimera 2* or the plasmid pYX232-*SCERV1*. Mitochondria were isolated from cells that were grown in selective medium without tryptophan and leucine containing 2% lactate and 0.5% galactose. For the Ni-NTA-agarose pull-down, mitochondria were solubilized in buffer containing 0.5% (w/v) Triton X-100 in buffer A (20 mM Tris, 80 mM KCl, 30 mM imidazole, 1 mM PMSF, pH 7.4) for 30 min at 4 °C. After a clarifying spin, solubilized material was incubated with 25 μL of Ni-NTA-agarose beads for 1 h. Following removal of the supernatant, beads were washed three times with buffer A containing 0.05% Triton X-100 and bound proteins were eluted with Laemmli buffer containing 300 mM imidazole. Total and elution fractions were then analyzed by SDS-PAGE and western blotting.

3. Results

3.1. ERV and small TIM1 cannot be deleted in L. infantum

Kinetoplastid parasites lack Mia40, which raises the question whether they can survive in the absence of Erv or putative substrates. In order to test the relevance of Erv in *Leishmania*, we tried to disrupt the encoding gene in the human pathogen *L. infantum* (locus LinJ.15.1020) by homologous recombination (Fig. 1A). Clonal heterozygous erv$^{+/-}$ strains were readily obtained after transfection of *L. infantum* promastigotes with plasmid pGL345-*LIERV* and selection with hygromycin as confirmed by PCR analysis (Fig. 1B). Growth curve analysis for liquid cultures of wild-type (wt) and erv$^{+/-}$ strains revealed no morphological abnormalities or drastic growth defects (Fig. 1C), and both strains had similar *Li*Erv protein levels (Fig. S1A). The second *LIERV* allele could not be deleted after subsequent transfection with plasmid pGL726-*LIERV* and selection with phleomycin, even after the introduction of an additional gene copy on plasmid pTEX-NEO-*LIERV* (Fig. 1B). The additional *LIERV* copy was functional as reflected by a drastic increase in the *Li*Erv protein concentration (Fig. S1A), which might explain the short lag phase and decreased maximum cell density for liquid cultures of erv$^{+/-}$ strains that carried the episomal *LIERV* copy when grown in the presence of the selection antibiotic G418 (Fig. 1C).

To exclude systematic methodological causes for the negative results regarding the generation of homozygous erv$^{-/-}$ knockout parasites, we performed parallel experiments for *LIsTIM1* (locus LinJ.25.1610) using the same knockout strategy with plasmids pGL345-*LIsTIM1* and pGL726-*LIsTIM1* (Fig. 1A). *Lis*Tim1, the homolog of the IMS marker protein small Tim1 from *L. tarentolae*, is a candidate substrate for oxidative protein folding in *Leishmania* mitochondria [42]. Heterozygous hygromycin-resistant stim$^{+/-}$ parasites revealed no abnormal morphology, drastic growth defects or altered protein levels compared to the wt strain (Fig. 1C, Fig. S1B). A homozygous stim$^{-/-}$ knockout strain was only obtained in the presence of an additional gene copy on plasmid pTEX-NEO-*LIsTIM1* (Fig. 1B). Again, complemented strains had a slight growth defect in the presence of G418 (Fig. 1C) and the protein concentration of *Lis*Tim1 was drastically up-regulated (Fig. S1B). The complemented stim$^{-/-}$ knockout strain neither lost its plasmid nor *Lis*Tim1 and remained resistant to G418 even after twelve months of

continuous culture in the absence of the selection drug, whereas a wt control strain lost the empty plasmid pTEX-NEO over time (Fig. 1D, Fig. S1B). Thus, small Tim1 is probably essential in promastigotes of *L. infantum*, indicating the importance of the oxidative folding pathway for parasite survival despite the absence of a Mia40 homolog. Repeated negative results for parallel *LIERV* knockout attempts with *LIsTIM1* as a control also support the interpretation that Erv is essential in *L. infantum*.

3.2. Chimeric LtErv can complement the loss of ScErv1

*Lt*Erv appears to function in *Leishmania* without a Mia40 homolog and, therefore, may require structural features that are incompatible with the oxidative protein folding system in yeast. To analyze which structure-function relationships might be relevant for the inability of *Lt*Erv to complement the loss of *Sc*Erv1 in yeast [43], we generated a set of chimeras. *Lt*Erv differs from *Sc*Erv1 in two major aspects, (i) the C-terminal addition of a kinetoplastida-specific second (KISS) domain and (ii) the position of two redox-active 'distal' or 'shuttle' cysteine residues at the C-terminal instead of the N-terminal arm (Fig. 2A). The shuttle cysteines transfer electrons to the conserved 'proximal' cysteines within the flavodomain [16,43]. To address the relevance of these structural elements, we either replaced the N-terminus before the Erv domain of *Lt*Erv with the N-terminal arm of *Sc*Erv1 (chimera 1–3) or the complete N-terminal half of *Lt*Erv with *Sc*Erv1 (chimera 4 and 5). A potential negative effect of the C-terminal arm or the KISS domain was addressed by systematically removing these structural elements in chimera 2, 3 and 5. Furthermore, to check whether the shuttle CQVYC-motif of *Lt*Erv is incompatible with the oxidative folding machinery in yeast, we replaced the CRSC-motif at the N-terminal arm of *Sc*Erv1 in chimera 6. The chimeric constructs were analyzed in complementation assays on agar plates with 5-fluoroorotic acid (FOA) for negative selection against the episomal copy of *SCERV1* in a haploid Δ*erv1* knockout strain (Fig. 2B). In contrast to the negative control, which was transformed with wild-type *LTERV*, viable yeast strains were obtained from FOA agar plates for all chimeras. The absence of *Sc*Erv1 and the presence of the chimeric proteins in yeast mitochondria were confirmed for at least three different clones of each construct-harboring strain by subcellular fractionation and western blot analysis (Fig. 2C, Fig. S2A). Furthermore, we confirmed the genotype for chimera 3 and 6 by analytic PCR (Fig. S2B).

Replacing the N-terminus of *Lt*Erv with the N-terminal arm of *Sc*Erv1 allowed *Lt*Erv to rescue the Δ*erv1* strain in complementation assays (Fig. 2B, Fig. S3A). Yeast cells with chimera 3 grew slowly but were viable, suggesting that the Erv domain of *Lt*Erv in combination with the N-terminal arm of *Sc*Erv1 is sufficient to be functional. Addition of the C-terminal arm and/or the KISS domain improved the growth of chimera 1 and 2, which was still not as good as the growth of the positive control with *Sc*Erv1. This suggests that the Erv domain of *Lt*Erv might not be able to fully replace the function of the endogenous Erv domain (Fig. S3A). Taking into account the improved growth of chimera 1 and 2 compared to chimera 3, it is unlikely that the KISS domain and the C-terminal arm have a deleterious effect on the function of *Lt*Erv in yeast. Complementation assays for chimera 4 and 5, in which the KISS domain alone or together with the C-terminal arm of *Lt*Erv were fused to the *Sc*Erv1 domain, also support the absence of a dominant-negative effect (Fig. 2B), for example, by inactivating Mia40. Furthermore, the CQVYC-motif of *Lt*Erv in chimera 6 could functionally replace the CRSC-motif at the N-terminal arm of *Sc*Erv1. Thus, the shuttle arm motif of *Lt*Erv is, at least in part, compatible with yeast Mia40. In summary, attachment of the N-terminal arm of *Sc*Erv1 to *Lt*Erv chimeras suffices to complement and rescue the Δ*erv1* strain. Neither the presence of the KISS domain or the C-terminal arm nor the shuttle cysteine motif of *Lt*Erv render the protein inactive and cause the incompatibility of *Lt*Erv with the oxidative folding machinery in yeast mitochondria.
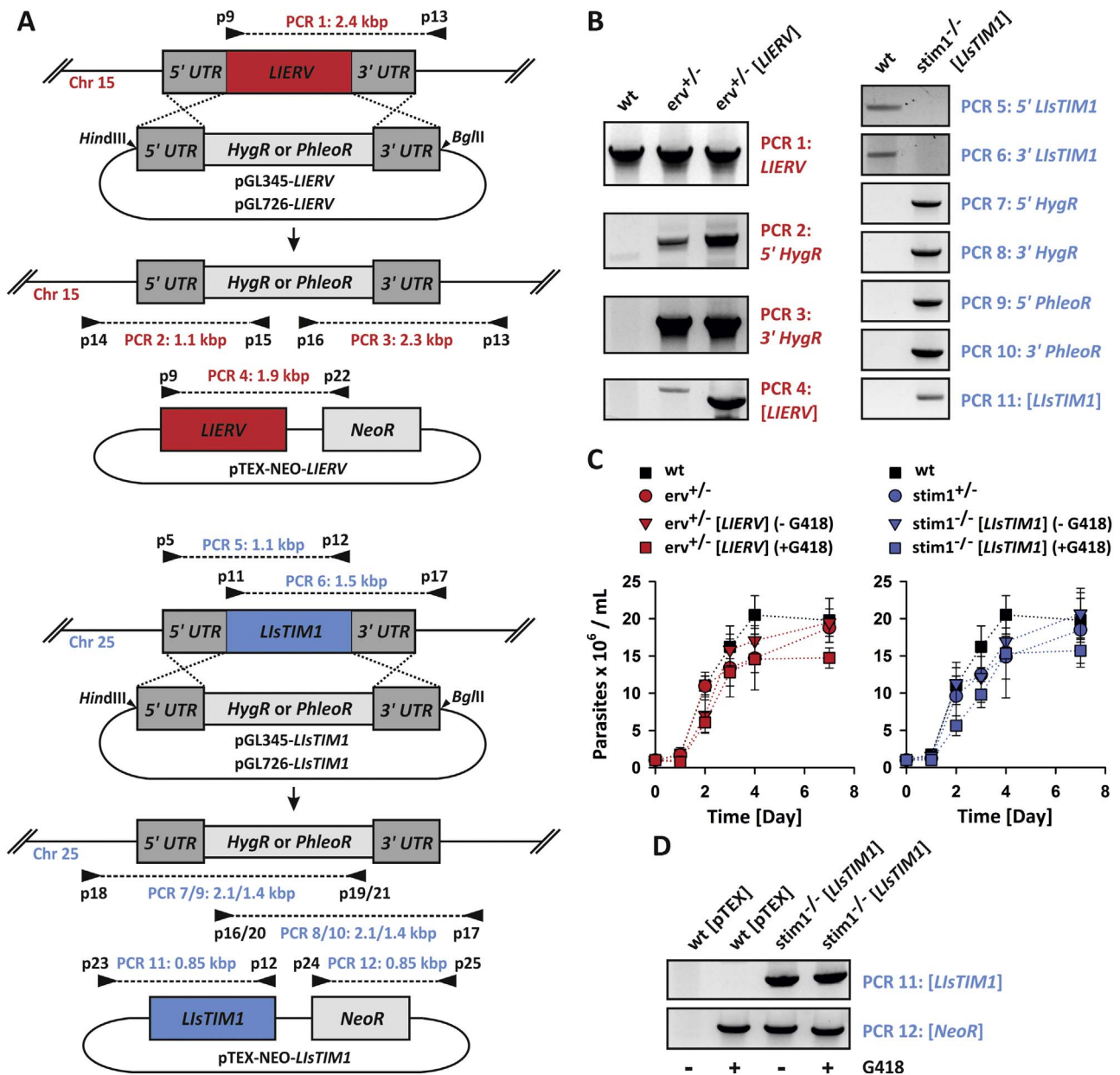
Fig. 1. *Knockout attempts for ERV and sTIM1 in Leishmania infantum.* (A) Schematic summary of the *LlERV* and *LlsTIM1* knockout strategy by homologous recombination using excised replacement cassettes from plasmids pGL345 and pGL726. Different selectable marker genes (*HygR* and *PhleoR*) were used in two rounds of transfection to target both alleles in diploid promastigotes. Experiments were performed with and without episomal copies of *LlERV* or *LlsTIM1* on rescue plasmid pTEX-NEO. Dashed lines indicate the sites of homologous recombination at the 5′ and 3′ untranslated regions (UTRs). Expected product sizes from analytic PCR reactions 1–12 are highlighted. (B) PCR analysis of the indicated parasite lines for (i) the absence or presence of chromosomal *LlERV* (PCR 1) and *LlsTIM1* (PCR 5 and 6), (ii) the 5′ and 3′ integration of the selectable marker genes (PCR 2, 3 and 7–10), and (iii) the absence or presence of episomal *LlERV* (PCR 4) or *LlsTIM1* (PCR 11). (C) Growth curve analysis for synchronized liquid cultures of the indicated parasite lines. Parasites that were complemented with an episomal copy of *LlERV* or *LlsTIM1* were grown with or without 50 μg/mL G418 (+/- G418). Values represent the mean and standard deviation of three independent biological replicates. (D) PCR analysis of the indicated parasite lines for the absence or presence of episomal *LlsTIM1* (PCR 11) or the pTEX-NEO selection marker *NeoR* (PCR 12) after twelve months of continuous culture in the absence or presence of 15 μg/mL G418.

### 3.3. Mutant LtErv^{C17S} can complement the loss of ScErv1

The chimera complementation assays suggested that *Lt*Erv can, at least in principle, functionally replace *Sc*Erv1. To further address the structural requirements for a successful complementation, we analyzed additional *Lt*Erv constructs in which we removed the N-terminal or C-terminal half of the protein (*Lt*Erv^{C-term} and *Lt*Erv^{N-term}) or replaced the different cysteine residues (Fig. 2D). Neither *Lt*Erv^{C-term} nor *Lt*Erv^{N-term} was able to complement the loss of *Sc*Erv1 (Fig. 2E, Fig. S3A). The latter result indicates that the flavodomain plus the N-terminal sequence of *Lt*Erv is not sufficient to complement for *Sc*Erv1 in yeast. It also excludes that the inability of full-length *Lt*Erv to complement is due to a

negative effect of the C-terminal half on its otherwise functional N-terminal half (in accordance with the growth of the truncated chimera in Fig. 2B). Systematic mutation of the distal, proximal, structural, and clamp cysteine residues of *Lt*Erv revealed that replacement of clamp residue Cys17 results in a functional mutant that was able to complement the loss of *Sc*Erv1 on FOA agar plates (Fig. 2E, Fig. S3A). The absence of *Sc*Erv1 and the presence of *Lt*Erv^{C17S} in yeast mitochondria were confirmed for different *LTERV*^{C17S} clones by subcellular fractionation and western blot analysis. Clones of all other *Lt*Erv mutants were either not viable or still contained *Sc*Erv1 (Fig. 2F, Fig. S4). Noteworthy, mutations of the distal cysteine residues in *Lt*Erv$^{C300S/C304S}$ or of one of the proximal cysteines in *Lt*Erv^{C63S} appeared to have no effect
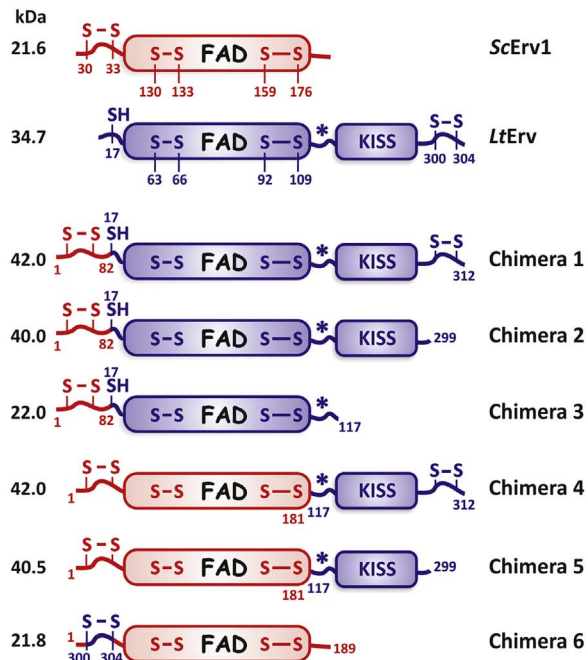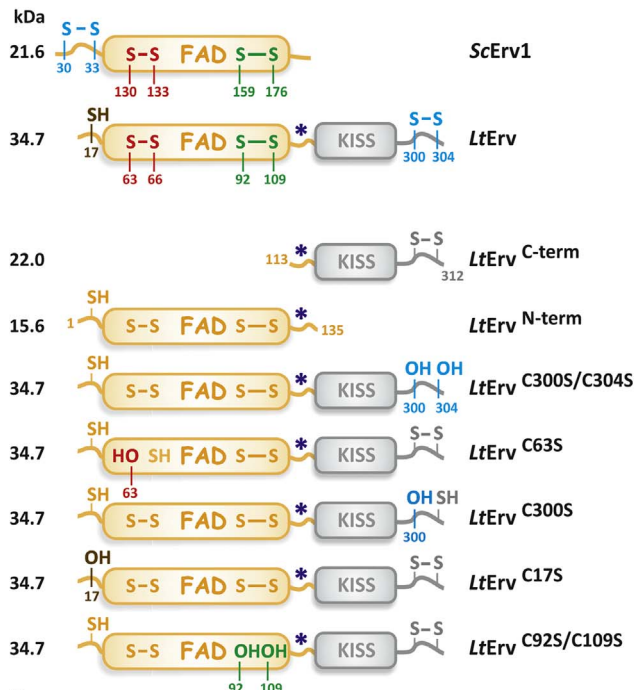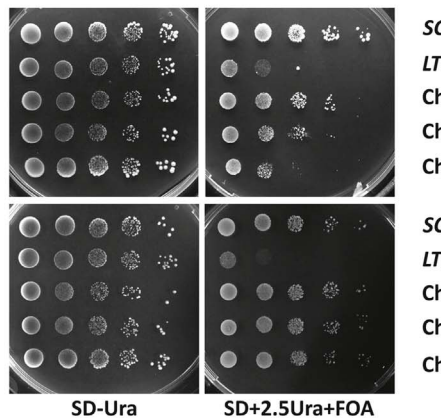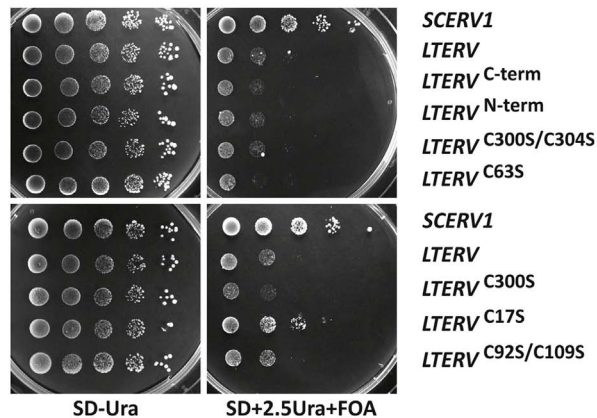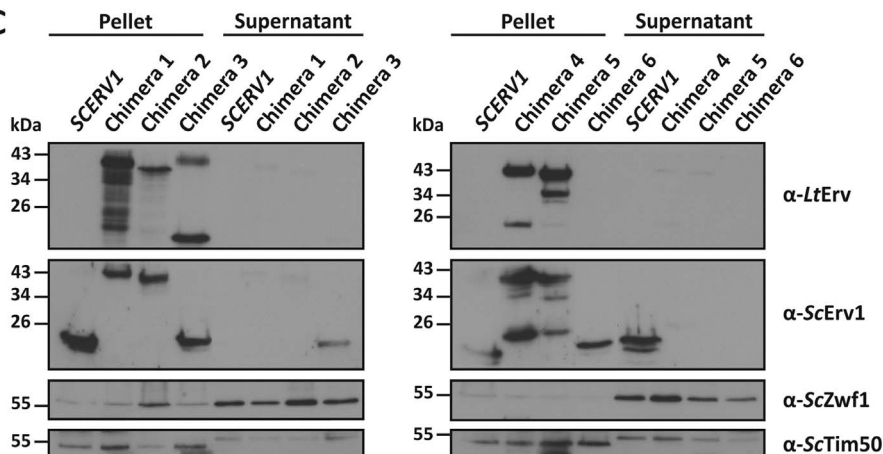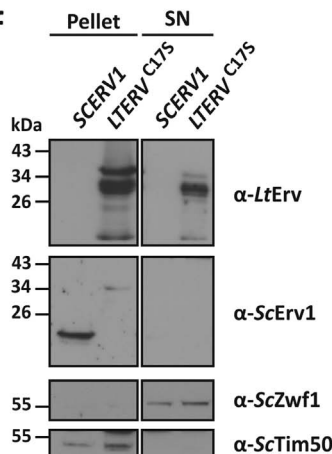
(caption on next page)

Fig. 2. *Yeast SCERV1 complementation assays with chimeric and mutant LTERV.* (A) Schematic summary of the constructs encoding *Sc*Erv1 (red), *Lt*Erv (purple) and the indicated chimera 1–6. The binding site for the peptide antibody α-*Lt*Erv [42] is marked with an asterisk. (B) A Δ*erv1* strain with an episomal copy of *SCERV1* on a *URA3*-containing rescue plasmid was subjected to plasmid shuffling in the presence of FOA after transfection with pYX232 plasmids that encode the indicated chimera. Copies of *SCERV1* and *LTERV* on plasmid pYX232 served as positive and negative controls, respectively [43]. Representative drop dilution assays (from left to right) on agar plates with or without FOA are shown for one of four independent biological replicates. (C) Western blot analyses of mitochondria-containing pellet fractions and cytosol-containing supernatant fractions of Δ*erv1* strains harboring the indicated chimera. Cytosolic glucose-6-phosphate dehydrogenase (*Sc*Zwf1) and mitochondrial *Sc*Tim50 served as controls. Expected molecular masses of the chimera are indicated in panel A. The western blots are representative for one clone of each construct (see also Fig. S2A). The absence of *Sc*Erv1 and presence of chimera 3 and 6 was also confirmed by analytic PCR (Fig. S2B). (D) Schematic summary of truncation constructs and cysteine mutants of *Lt*Erv. (E) Plasmid shuffling experiments with mutant *LTERV* as in panel B. (F) Cell fractionation of a Δ*erv1* strain that was complemented with *LTERV^{C17S}* as in panel C (see also Fig. S4). SN, supernatant.

on the mitochondrial localization of the proteins, whereas *Lt*Erv^{C17S} was also found in the cytosolic fraction.

In order to test whether the presence of Cys17 might have masked a positive complementation for the other *Lt*Erv mutants, we repeated the *SCERV1* complementation experiments with the C17S constructs *Lt*Erv^{N-term/C17S}, *Lt*Erv^{C17S/C63S}, *Lt*Erv^{C17S/C300S}, *Lt*Erv^{C17S/C300S/C304S}, and *Lt*Erv^{C17S/C92S/C109S}. However, none of these constructs could complement the loss of *Sc*Erv1 (Fig. S5).

In summary, Cys17 renders *Lt*Erv non-functional in the yeast system, and the presence of this cysteine residue is, at least in part, the cause for the incompatibility between *Lt*Erv and the oxidative folding machinery in yeast mitochondria. Replacing either residue Cys17 with serine or residues 1–16 of *Lt*Erv with the N-terminus of *Sc*Erv1 in chimera 1–3 partially rescues the functionality of *Lt*Erv and its compatibility with the yeast system.

3.4. LtErv^{C17S} and chimera 1, 2 and 6 have specific carbon source-dependent growth defects

To further characterize the complemented yeast strains, we compared their growth in liquid or on agar minimal medium with glucose (SD), galactose (SGal) or glycerol (SG) as a carbon source (Fig. 3 and Fig. S6). Chimera 1 had a pronounced growth defect on all three carbon sources. This phenotype was observed in liquid medium and on agar plates. In contrast, chimera 2 showed a growth defect in SG liquid medium but not in SGal or SD medium. Chimera 2 also grew normal on SG agar plates. Chimera 3 revealed no striking phenotype, whereas chimera 4 and 5 grew slightly faster on SGal and SG agar plates than the control. This phenotype was absent in liquid medium. Chimera 6 revealed a growth defect on SG agar plates and in SD liquid medium. Cells with *Lt*Erv^{C17S} grew normally in SD medium but reached a much lower
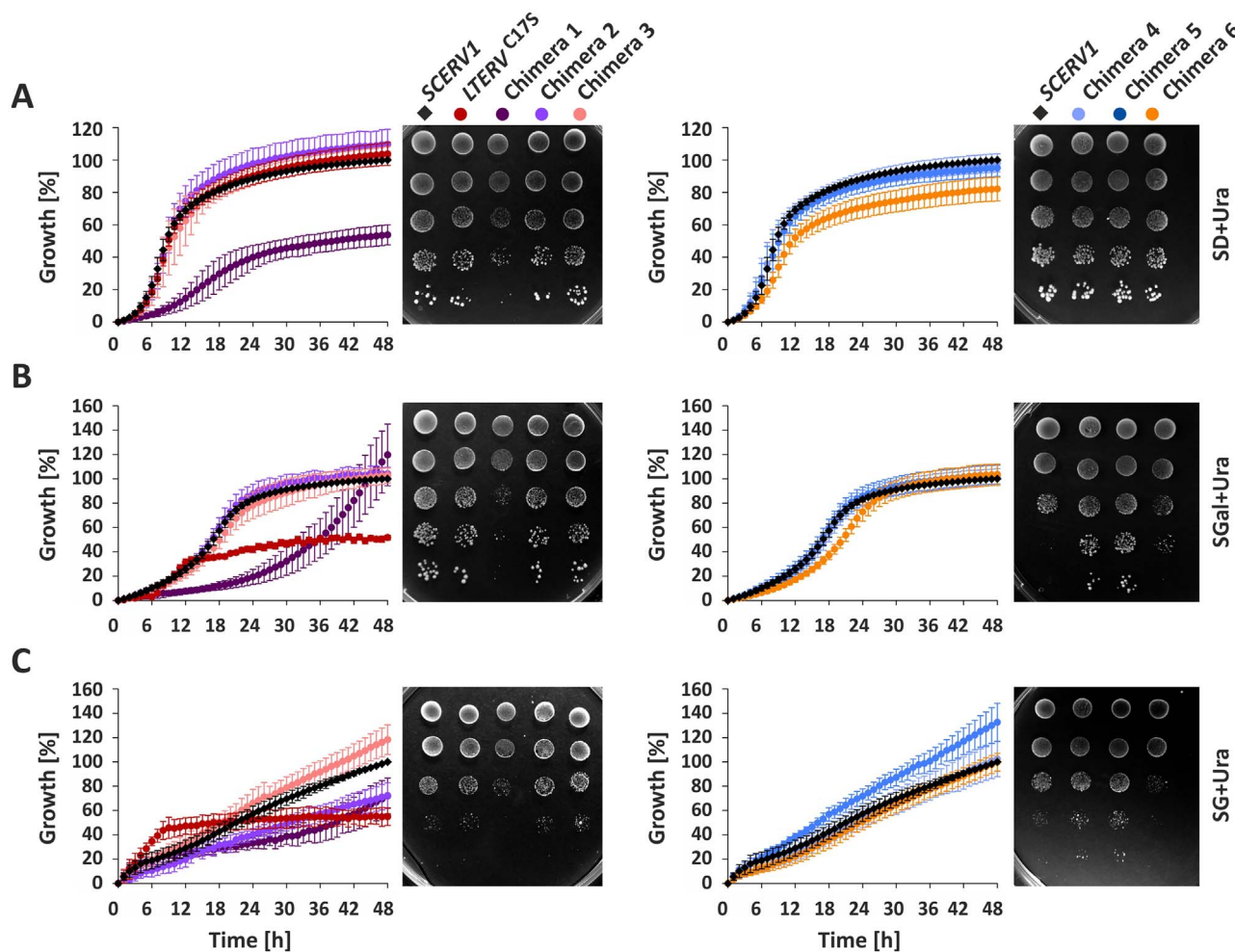
Fig. 3. *Growth assays of complemented Δerv1 strains.* Yeast strains harboring *Chimera 1–6* or *LTERV^{C17S}* were analyzed in liquid medium and on agar plates. (A) Growth on minimal medium with 2% glucose as a carbon source (SD). (B) Growth on 3% galactose medium (SGal). (C) Growth on 3% glycerol medium (SG). Growth curves in liquid medium were normalized to the growth of the Δ*erv1* strain harboring an episomal copy of *SCERV1* on plasmid pYX232. Values in liquid medium represent the mean and standard deviation of three to five independent biological replicates. Representative drop dilution assays (from top to bottom) on agar plates on day 3 (SD), day 5 (SGal) and day 8 (SG) are shown for one of three to four independent biological replicates. The phenotypes were confirmed for two or three different clones for each construct.
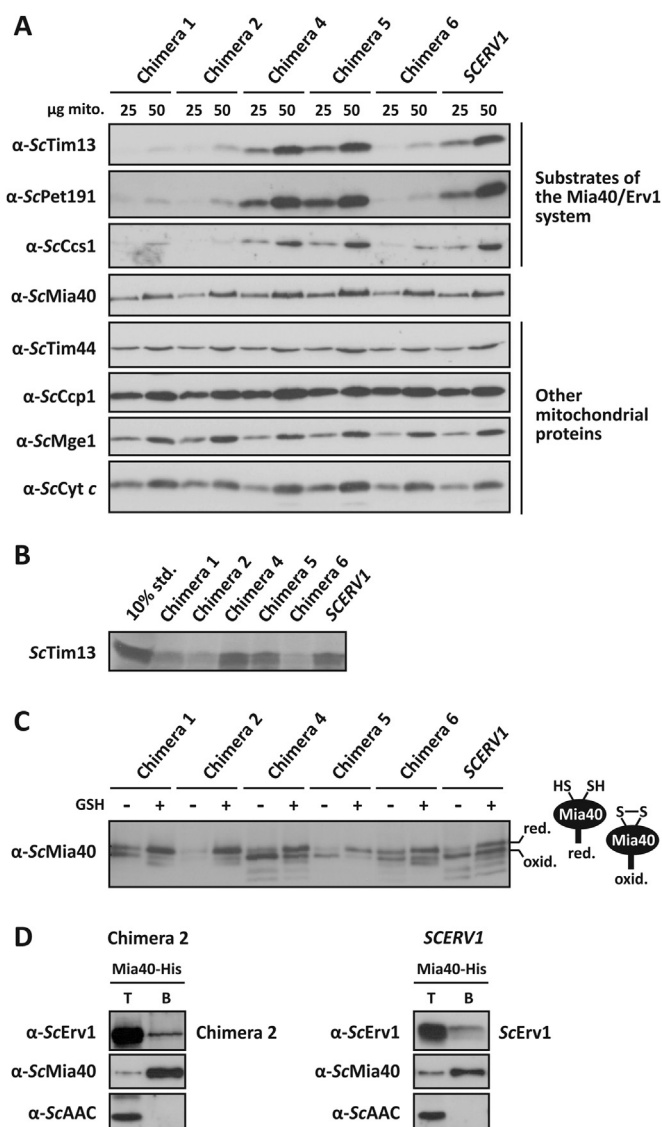
Fig. 4. *Functional analysis of LtErv chimera in yeast.* (A) Western blot analysis of steady-state protein levels in mitochondrial preparations that contain the indicated chimera or *Sc*Erv1 as a control. The twin Cx$_3$C protein *Sc*Tim13, the twin Cx$_9$C cytochrome c oxidase assembly factor *Sc*Pet191, and the copper chaperone for superoxide dismutase *Sc*Ccs1 represent different substrate classes of the Mia40/Erv1 system [15,21–24]. *Sc*Tim44 and the co-chaperone *Sc*Mge1 contain a pre-sequence and are imported into the mitochondrial matrix, whereas the IMS proteins cytochrome *c* and cytochrome *c* peroxidase *Sc*Ccp1 are imported independent of the Mia40/Erv1 system. (B) *In vitro* protein import of [^{35}S]-methionine-labeled *Sc*Tim13 into isolated mitochondria harboring the indicated chimera or *Sc*Erv1 as a control. Ten percent of the labeled protein served as a loading control (10% std.). (C) Western blot analysis of the redox state of *Sc*Mia40 in isolated mitochondria that contain the indicated chimera or *Sc*Erv1 as a control. Mitochondria were treated with or without 5 mM GSH before protein separation by non-reducing SDS-PAGE. Red., reduced; oxid., oxidized. (D) Co-isolation of chimera 2 with His-tagged *Sc*Mia40. Mitochondrial lysates were prepared from strains containing His-tagged *Sc*Mia40 and episomally encoded chimera 2 or *Sc*Erv1. The mitochondrial lysates were incubated with Ni-NTA beads and the beads were isolated. Total proteins, T (15%), and bound material, B (100%), were analyzed by SDS-PAGE and immunoblotting with antibodies against *Sc*Erv1, *Sc*Mia40 and the ATP/ADP-carrier (*Sc*AAC).

final cell density in SGal or SG liquid medium. Noteworthy, the strain grew faster during the initial 12 h in SG medium than the control. The phenotype of *Lt*Erv^{C17S} was specific for liquid medium and was absent on agar plates. The different phenotypes for *Lt*Erv^{C17S} on SD and SGal medium are quite surprising taking into account that galactose is converted to glucose-6-phosphate by the Leloir pathway [58], which should not be directly affected by the mitochondria. In summary,

pronounced growth defects on SG medium for chimera 1 and 2 in liquid medium as well as for chimera 6 on agar plates point towards an impaired mitochondrial respiration in these strains.

### 3.5. Chimera 1, 2 and 6 have an impaired oxidative folding pathway

Analysis of the substrates of the Mia40/Erv1 system by western blotting revealed reduced steady-state protein levels in mitochondria with chimera 1, 2 and 6 compared to control mitochondria with *Sc*Erv1 (Fig. 4A). In contrast, mitochondria with chimera 4 and 5 had normal steady-state substrate concentrations. The results suggest that the CRSC-motif of *Sc*Erv1 has been optimized for the interaction with *Sc*Mia40 and/or the *Sc*Erv1 flavodomain during the course of evolution, as reflected by chimera 6, which functions with a decreased efficiency compared to the control. Furthermore, the N-terminal arm of *Sc*Erv1 and the proximal cysteines of the flavodomain of *Lt*Erv in chimera 1 and 2 are not perfectly compatible.

The altered steady-state concentrations were specific for class II IMS proteins, which are oxidatively trapped [2]. Other mitochondrial proteins were not affected by the chimeras (Fig. 4A). This also includes *Sc*Mia40 itself, which has an N-terminal mitochondrial targeting signal and a transmembrane segment that is inserted into the inner mitochondrial membrane by the TIM23 complex before *Sc*Mia40 is oxidatively folded by the Mia40/Erv1 system [11,12,18,25,59]. An impaired protein import of the class II reference protein *Sc*Tim13 was confirmed using *in vitro* import assays (Fig. 4B). Again, mitochondria with chimera 1, 2 and 6, but not with chimera 4 and 5, imported less *Sc*Tim13 compared to mitochondria with *Sc*Erv1.

The underlying cause for the impaired protein import of class II proteins was presumably the altered ratio between reduced and oxidized *Sc*Mia40, as revealed by redox mobility shift assays and western blot analysis (Fig. 4C). The redox state of *Sc*Mia40 from isolated mitochondria with chimera 1, 2 and 6 was shifted to the reduced state compared to the redox state of *Sc*Mia40 from mitochondria with *Sc*Erv1 or chimera 4 and 5, which were predominantly oxidized. Thus, oxidation of *Sc*Mia40 by *Sc*Erv1 or chimera 4 and 5 is probably more efficient than the oxidation of *Sc*Mia40 by chimera 1, 2 and 6. This interpretation is also supported when isolated mitochondria were challenged with GSH. GSH treatment yielded almost completely reduced *Sc*Mia40 for chimera 1 and 2 in contrast to mitochondria with chimera 4 or *Sc*Erv1 (Fig. 4C).

Oxidation of *Sc*Mia40 by *Sc*Erv1 requires the physical interaction of both proteins. We previously showed that *Lt*Erv cannot replace *Sc*Erv1 and that wild type *Lt*Erv does not interact with *Sc*Mia40 [43]. Taking into account that an attachment of the N-terminal arm of *Sc*Erv1 to the flavodomain of *Lt*Erv rescued the deletion of *SCERV1* (Fig. 2), we tested an interaction with *Sc*Mia40 for one of these chimera in a Ni-NTA pull-down experiment. Indeed, His-tagged *Sc*Mia40 co-precipitated with chimera 2, albeit with reduced efficiency compared to *Sc*Erv1 (Fig. 4D). As negative control, a hydrophobic inner membrane protein, the ATP/ADP carrier, was not co-precipitated, indicating the specificity of the pull-down experiment. The experiment supports the hypothesis that the N-terminal arm of *Sc*Erv1 of the chimera oxidizes *Sc*Mia40 and subsequently transfers the electrons to the flavodomain of *Lt*Erv. However, the functionality of the N-terminal arm of *Sc*Erv1 appears to be impaired by the presence of the flavodomain of *Lt*Erv, which shifts the steady-state equilibrium between oxidized and reduced *Sc*Mia40 towards the reduced form.

In summary, oxidation of *Sc*Mia40 by chimera 1, 2 and 6 appears to be less efficient than oxidation by chimera 4 and 5. The subsequent increase of reduced *Sc*Mia40 in mitochondria with chimera 1, 2 and 6 most likely impairs the import of substrates of the Mia40/Erv1 system *in vitro* and *in vivo* and results in decreased levels of these proteins in mitochondria.
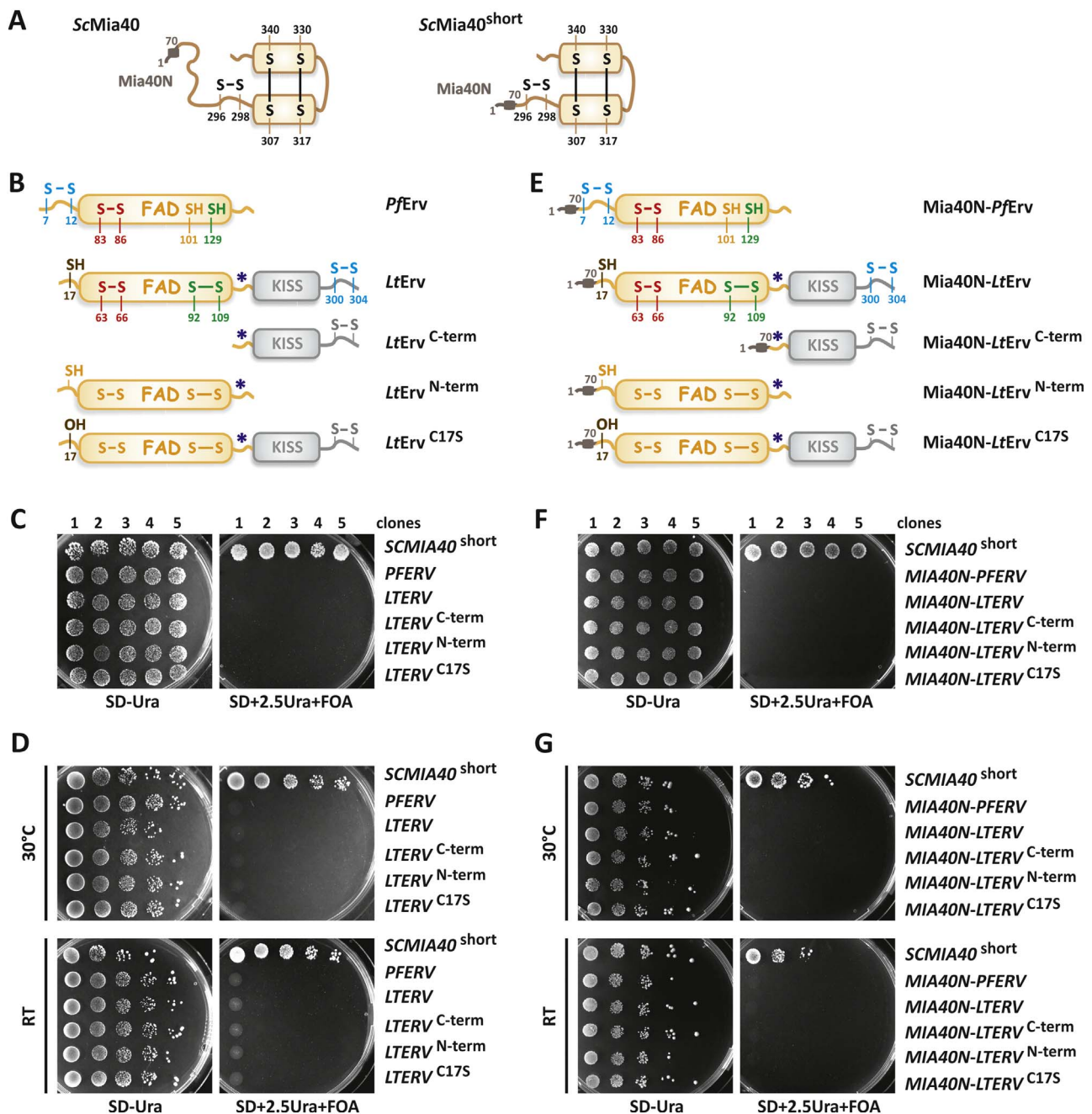
Fig. 5. *Yeast SCMIA40 complementation assays with truncated and mutant LTERV.* (A) Schematic summary of full length and truncated *Sc*Mia40[short] with the N-terminal mitochondrial targeting signal and transmembrane segment (Mia40N) and disulfide bonds highlighted. (B) Schematic summary of the constructs encoding *Pf*Erv as well as full length, truncated or mutant *Lt*Erv. (C) A Δ*mia40* strain with an episomal copy of *SCMIA40* on a *URA3*-containing rescue plasmid was subjected to plasmid shuffling in the presence of FOA after transfection with pYX232 plasmids that encode the indicated parasite Erv constructs. The complementation with *SCMIA40*[short] served as a positive control. (D) The complementation assays were also repeated in parallel as drop dilution assays at 30 °C and room temperature (RT). Representative drop dilution assays (from left to right) on agar plates with or without FOA are shown for one of three independent biological replicates. (E) Schematic summary of the constructs encoding Mia40N-tagged *Pf*Erv as well full length, truncated or mutant *Lt*Erv. (F) and (G) Complementation assays with Mia40N-tagged constructs.

3.6. LtErv cannot functionally replace yeast Mia40

Our results show that the KISS domain does not interfere with the function of *Lt*Erv in yeast. A potential function of the KISS domain, which lacks a cysteine residue [43], might be the recruitment of protein thiol substrates before they interact with the shuttle disulfide. Thus, the KISS domain and the shuttle arm might functionally replace Mia40, which does not only introduce disulfide bonds but also serves as a receptor and binds to a hydrophobic patch of the imported substrate [26,28,29,31,49,60–63]. To test the hypothesis whether protist Erv homologs are able to replace Mia40, we tried to complement a Δ*mia40*

strain with genes encoding the Erv homolog from *P. falciparum* (which lacks a KISS domain), full length *Lt*Erv, *Lt*Erv[C-term], *Lt*Erv[N-term], and *Lt*Erv[C17S] (Fig. 5). Negative selection on FOA agar plates against the episomal copy of a short functional version of *SCMIA40* in the Δ*mia40* knockout strain revealed that none of the constructs could complement the loss of *Sc*Mia40 (Fig. 5C). This was also the case when alternative temperatures were tested (Fig. 5D, Fig. S3B).

In a subsequent set of experiments, we fused the N-terminal mitochondrial targeting signal and transmembrane segment of *Sc*Mia40 to our protist Erv constructs in order to localize the proteins to the same location in the inner mitochondrial membrane as endogenous *Sc*Mia40

(Fig. 5E). However, none of these Mia40N-fusion constructs was able to complement the loss of *Sc*Mia40 (Fig. 5F,G). In a last set of experiments, we addressed the hypothesis whether some of the chimeric *Lt*Erv constructs from Fig. 2 have a Mia40-like activity. We therefore tested chimera 1–6 as well as their fusion constructs with the N-terminal mitochondrial targeting signal and transmembrane segment of *Sc*Mia40 in *SCMIA40* complementation assays. Again, none of the twelve constructs could complement the loss of *Sc*Mia40 (Fig. S7). In summary, neither *Pf*Erv nor *Lt*Erv or structural elements of *Lt*Erv, such as the KISS domain and the C-terminal arm, can functionally replace *Sc*Mia40.

4. Discussion

Our knockout studies for *LlERV* and *LlsTIM1* suggest that both genes are essential for parasite survival and underline the potential of mitochondrial protein import pathways for future intervention strategies against important pathogens. An analogous knockout strategy has been previously used to show that a cytosolic tryparedoxin is essential for *L. infantum* survival [64]. Furthermore, RNAi studies in the related kinetoplastid parasite *T. brucei* suggested that *Tb*Erv is essential [44,45,65]. Nevertheless, we are aware that viable knockout strains with a drastic growth defect can be missed without negative selection and that the recent establishment of CRISPR/Cas9 systems in *Leishmania* [66–68] could be extremely helpful to get a definite answer regarding the essentiality of Erv and sTim1 in *Leishmania* pathogens.

Previous studies on Erv homologs from human, yeast, *L. tarentolae*, *T. brucei*, and *Arabidopsis thaliana* revealed that the redox-active shuttle cysteines are present in highly variable motifs, which are sometimes close to the N- or the C-terminus [30,37,43,44,69–73]. Wild-type Erv homologs from *A. thaliana* and *L. tarentolae* both carry a C-terminal shuttle arm and were unable to complement the loss of *Sc*Erv1 [43,72]. Even though complementation with *Lt*Erv^{C17S} resulted in a growth defect on FOA agar plates, the viability of the strain clearly shows that the position of the shuttle arm is not a criterion for exclusion for the functionality in yeast. This is also the case regarding the CRSC shuttle arm motif, which was successfully replaced in chimera 6, although at the cost of a drastically impaired mitochondrial protein import. Residue Cys17 of *Lt*Erv is partially conserved in Erv homologs [16,43] and was shown to form a clamp disulfide bond in mammalian ALR [33,37,74]. Notably, heterologous human ALR was found in the yeast cytosol and was unable to functionally replace *Sc*Erv1 unless a bipartite pre-sequence was fused to its N-terminus or residues 1–80 of ALR were replaced with residues 1–93 of *Sc*Erv1 [75,76]. How residue Cys17 of *Lt*Erv exactly impairs its function in yeast and whether this neglected residue exerts a physiological function in a subset of Erv homologs remains to be studied. Chimera 1 and 4 both contain an N- and C-terminal shuttle arm, but only yeast cells with chimera 1 had a growth defect. Maybe both shuttle arms compete for the proximal cysteines of the flavodomain of chimera 1 or form long-lived disulfide-bonded intermediates in contrast to chimera 4. In summary, growth and import defects for chimera 1, 2 and 6 suggest that the shuttle arm motif and the interactions between the shuttle arm and the flavodomain and/or Mia40 have been optimized for different Erv homologs in the course of evolution. Nevertheless, the mitochondrial protein import machinery in yeast is robust enough to allow certain degrees of incompatibility.

Can protist Erv homologs act alone and do protists have simplified oxidative folding machineries mediating the IMS protein import as recently suggested [65,77]? This possibility would require an efficient interaction of *Leishmania* class II IMS proteins with *Lt*Erv, including their direct oxidation by *Lt*Erv. In this case one might expect that *Lt*Erv is able to complement the function of *Sc*Mia40, because the import signals of IMS proteins are functionally conserved in the course of evolution [42]. Our complementation studies do not provide evidence for a simplified oxidation and folding machinery, because neither the KISS domain nor full length *Lt*Erv, *Lt*Erv^{C17S}, *Lt*Erv^{C-term} or chimera 1–6 could rescue the Δ*mia40* strain. This rather points to the presence of a

Mia40 replacement in protists (compound Z in one of our previously discussed evolutionary scenarios [42]). Such a model suggests that protists without Mia40 have a replacement for this substrate receptor. So far we were unable to identify a stable disulfide-bonded interaction partner between *Lt*Erv and another protein in *Leishmania* mitochondria using a variety of experimental approaches (Liedgens et al., unpublished). However, just because redox mobility shift assays and pull-down experiments do not reveal a stable interaction, we cannot exclude a transient or non-covalent interaction with a Mia40 replacement. The "sluggish" behavior of *Sc*Mia40 with its metastable intermolecular disulfide species is actually rather an exception compared to oxidative protein folding in the periplasm or the endoplasmic reticulum [7,31]. What could be a reasonable replacement of Mia40? A recent study showed that a subpopulation of the yeast peroxidase GPx3 interacts with *Sc*Mia40 and the oxidative folding pathway in the IMS [78]. This situation somehow resembles the transient interaction between peroxiredoxin IV and protein disulfide isomerase (PDI) for oxidative protein folding in the endoplasmic reticulum of mammals [79,80]. A tryparedoxin peroxidase (Tb927.9.5750) was also identified in a pull-down assay with *Tb*Erv [65], and this protein was 1.34-fold up-regulated in the *Tb*Erv knockdown strain [45]. Whether this is just a false positive hit due to the high abundance of the cytosolic peroxidase or points to a dual localization and alternative function in oxidative protein folding remains to be studied. However, GPx3 and peroxiredoxin IV are both downstream electron acceptors of Mia40 and PDI so that an analogous involvement of the tryparedoxin peroxidase in the IMS of kinetoplastid parasites would still necessitate the existence of an alternative receptor for the incoming protein substrates. Further studies are obviously necessary to identify the receptor for incoming IMS proteins and to decipher the oxidative folding machineries in protist mitochondria.

Appendix A. Supplementary material

Supplementary data associated with this article can be found in the online version at http://dx.doi.org/10.1016/j.redox.2017.12.010.

References

[1] N. Wiedemann, N. Pfanner, Mitochondrial machineries for protein import and assembly, Annu. Rev. Biochem. 86 (2017) 685–714.

[2] J.M. Herrmann, K. Hell, Chopped, trapped or tacked–protein translocation into the IMS of mitochondria, Trends Biochem. Sci. 30 (2005) 205–211.

[3] S. Longen, M. Bien, K. Bihlmaier, C. Kloeppel, F. Kauff, M. Hammermeister, B. Westermann, J.M. Herrmann, J. Riemer, Systematic analysis of the twin cx(9)c protein family, J. Mol. Biol. 393 (2009) 356–368.

[4] F.N. Vogtle, J.M. Burkhart, S. Rao, C. Gerbeth, J. Hinrichs, J.C. Martinou, A. Chacinska, A. Sickmann, R.P. Zahedi, C. Meisinger, Intermembrane space proteome of yeast mitochondria, Mol. Cell. Proteom.: MCP. 11 (2012) 1840–1852.

[5] V. Hung, P. Zou, H.W. Rhee, N.D. Udeshi, V. Cracan, T. Svinkina, S.A. Carr, V.K. Mootha, A.Y. Ting, Proteomic mapping of the human mitochondrial intermembrane space in live cells via ratiometric APEX tagging, Mol. Cell 55 (2014) 332–341.

[6] L. MacPherson, K. Tokatlidis, Protein trafficking in the mitochondrial

intermembrane space: mechanisms and links to human disease, Biochem. J. 474 (2017) 2533–2545.

[7] A.J. Erdogan, J. Riemer, Mitochondrial disulfide relay and its substrates: mechanisms in health and disease, Cell Tissue Res. 367 (2017) 59–72.

[8] F.U. Hartl, J. Ostermann, B. Guiard, W. Neupert, Successive translocation into and out of the mitochondrial matrix: targeting of proteins to the intermembrane space by a bipartite signal peptide, Cell 51 (1987) 1027–1037.

[9] A. Schneider, M. Behrens, P. Scherer, E. Pratje, G. Michaelis, G. Schatz, Inner membrane protease I, an enzyme mediating intramitochondrial protein sorting in yeast, EMBO J. 10 (1991) 247–254.

[10] B.S. Glick, A. Brandt, K. Cunningham, S. Muller, R.L. Hallberg, G. Schatz, Cytochromes c1 and b2 are sorted to the intermembrane space of yeast mitochondria by a stop-transfer mechanism, Cell 69 (1992) 809–822.

[11] A. Chacinska, S. Pfannschmidt, N. Wiedemann, V. Kozjak, L.K. Sanjuan Szklarz, A. Schulze-Specking, K.N. Truscott, B. Guiard, C. Meisinger, N. Pfanner, Essential role of Mia40 in import and assembly of mitochondrial intermembrane space proteins, EMBO J. 23 (2004) 3735–3746.

[12] M. Naoe, Y. Ohwa, D. Ishikawa, C. Ohshima, S. Nishikawa, H. Yamamoto, T. Endo, Identification of Tim40 that mediates protein sorting to the mitochondrial intermembrane space, J. Biol. Chem. 279 (2004) 47815–47821.

[13] N. Mesecke, N. Terziyska, C. Kozany, F. Baumann, W. Neupert, K. Hell, J.M. Herrmann, A disulfide relay system in the intermembrane space of mitochondria that mediates protein import, Cell 121 (2005) 1059–1069.

[14] S. Hofmann, U. Rothbauer, N. Muhlenbein, K. Baiker, K. Hell, M.F. Bauer, Functional and mutational characterization of human MIA40 acting during import into the mitochondrial intermembrane space, J. Mol. Biol. 353 (2005) 517–528.

[15] N. Terziyska, T. Lutz, C. Kozany, D. Mokranjac, N. Mesecke, W. Neupert, J.M. Herrmann, K. Hell, Mia40, a novel factor for protein import into the intermembrane space of mitochondria is able to bind metal ions, FEBS Lett. 579 (2005) 179–184.

[16] M. Deponte, K. Hell, Disulphide bond formation in the intermembrane space of mitochondria, J. Biochem. 146 (2009) 599–608.

[17] M. Fischer, S. Horn, A. Belkacemi, K. Kojer, C. Petrungaro, M. Habich, M. Ali, V. Kuttner, M. Bien, F. Kauff, J. Dengjel, J.M. Herrmann, J. Riemer, Protein import and oxidative folding in the mitochondrial intermembrane space of intact mammalian cells, Mol. Biol. Cell 24 (2013) 2160–2170.

[18] N. Terziyska, B. Grumbt, M. Bien, W. Neupert, J.M. Herrmann, K. Hell, The sulfhydryl oxidase Erv1 is a substrate of the Mia40-dependent protein translocation pathway, FEBS Lett. 581 (2007) 1098–1102.

[19] K. Gabriel, D. Milenkovic, A. Chacinska, J. Muller, B. Guiard, N. Pfanner, C. Meisinger, Novel mitochondrial intermembrane space proteins as substrates of the MIA import pathway, J. Mol. Biol. 365 (2007) 612–620.

[20] E. Kallergi, M. Andreadaki, P. Kritsiligkou, N. Katrakili, C. Pozidis, K. Tokatlidis, L. Banci, I. Bertini, C. Cefaro, S. Ciofi-Baffoni, K. Gajda, R. Peruzzini, Targeting and maturation of Erv1/ALR in the mitochondrial intermembrane space, ACS Chem. Biol. 7 (2012) 707–714.

[21] S. Reddehase, B. Grumbt, W. Neupert, K. Hell, The disulfide relay system of mitochondria is required for the biogenesis of mitochondrial Ccs1 and Sod1, J. Mol. Biol. 385 (2009) 331–338.

[22] D.P. Gross, C.A. Burgard, S. Reddehase, J.M. Leitch, V.C. Culotta, K. Hell, Mitochondrial Ccs1 contains a structural disulfide bond crucial for the import of this unconventional substrate by the disulfide relay system, Mol. Biol. Cell. 22 (2011) 3758–3767.

[23] C. Kloppel, Y. Suzuki, K. Kojer, C. Petrungaro, S. Longen, S. Fiedler, S. Keller, J. Riemer, Mia40-dependent oxidation of cysteines in domain I of Ccs1 controls its distribution between mitochondria and the cytosol, Mol. Biol. Cell 22 (2011) 3749–3757.

[24] P. Bragoszewski, A. Gornicka, M.E. Sztolsztener, A. Chacinska, The ubiquitin-proteasome system regulates mitochondrial intermembrane space proteins, Mol. Cell. Biol. 33 (2013) 2136–2148.

[25] B. Grumbt, V. Stroobant, N. Terziyska, L. Israel, K. Hell, Functional characterization of Mia40p, the central component of the disulfide relay system of the mitochondrial intermembrane space, J. Biol. Chem. 282 (2007) 37461–37470.

[26] S. Kawano, K. Yamano, M. Naoe, T. Momose, K. Terao, S. Nishikawa, N. Watanabe, T. Endo, Structural basis of yeast Tim40/Mia40 as an oxidative translocator in the mitochondrial intermembrane space, Proc. Natl. Acad. Sci. USA 106 (2009) 14403–14407.

[27] N. Terziyska, B. Grumbt, C. Kozany, K. Hell, Structural and functional roles of the conserved cysteine residues of the redox-regulated import receptor Mia40 in the intermembrane space of mitochondria, J. Biol. Chem. 284 (2009) 1353–1363.

[28] L. Banci, I. Bertini, C. Cefaro, S. Ciofi-Baffoni, A. Gallo, M. Martinelli, D.P. Sideris, N. Katrakili, K. Tokatlidis, MIA40 is an oxidoreductase that catalyzes oxidative protein folding in mitochondria, Nat. Struct. Mol. Biol. 16 (2009) 198–206.

[29] L. Banci, I. Bertini, C. Cefaro, L. Cenacchi, S. Ciofi-Baffoni, I.C. Felli, A. Gallo, L. Gonnelli, E. Luchinat, D. Sideris, K. Tokatlidis, Molecular chaperone function of Mia40 triggers consecutive induced folding steps of the substrate in mitochondrial protein import, Proc. Natl. Acad. Sci. USA 107 (2010) 20190–20195.

[30] M. Bien, S. Longen, N. Wagener, I. Chwalla, J.M. Herrmann, J. Riemer, Mitochondrial disulfide bond formation is driven by intersubunit electron transfer in Erv1 and proofread by glutathione, Mol. Cell 37 (2010) 516–528.

[31] J.R. Koch, F.X. Schmid, Mia40 targets cysteines in a hydrophobic environment to direct oxidative protein folding in the mitochondria, Nat. Commun. 5 (2014) 3041.

[32] S. Allen, V. Balabanidou, D.P. Sideris, T. Lisowsky, K. Tokatlidis, Erv1 mediates the Mia40-dependent protein import pathway and provides a functional link to the respiratory chain by shuttling electrons to cytochrome c, J. Mol. Biol. 353 (2005) 937–944.

[33] S.R. Farrell, C. Thorpe, Augmenter of liver regeneration: a flavin-dependent sulfhydryl oxidase with cytochrome c reductase activity, Biochemistry 44 (2005) 1532–1541.

[34] M. Rissler, N. Wiedemann, S. Pfannschmidt, K. Gabriel, B. Guiard, N. Pfanner, A. Chacinska, The essential mitochondrial protein Erv1 cooperates with Mia40 in biogenesis of intermembrane space proteins, J. Mol. Biol. 353 (2005) 485–492.

[35] K. Bihlmaier, N. Mesecke, N. Terziyska, M. Bien, K. Hell, J.M. Herrmann, The disulfide relay system of mitochondria is connected to the respiratory chain, J. Cell Biol. 179 (2007) 389–395.

[36] D.V. Dabir, E.P. Leverich, S.K. Kim, F.D. Tsai, M. Hirasawa, D.B. Knaff, C.M. Koehler, A role for cytochrome c and cytochrome c peroxidase in electron shuttling from Erv1, EMBO J. 26 (2007) 4801–4811.

[37] L. Banci, I. Bertini, V. Calderone, C. Cefaro, S. Ciofi-Baffoni, A. Gallo, E. Kallergi, E. Lionaki, C. Pozidis, K. Tokatlidis, Molecular recognition and substrate mimicry drive the electron-transfer process between MIA40 and ALR, Proc. Natl. Acad. Sci. USA 108 (2011) 4811–4816.

[38] S.E. Neal, D.V. Dabir, J. Wijaya, C. Boon, C.M. Koehler, Osm1 facilitates the transfer of electrons from Erv1 to fumarate in the redox-regulated import pathway in the mitochondrial intermembrane space, Mol. Biol. Cell 28 (2017) 2773–2785.

[39] S.M. Adl, A.G. Simpson, C.E. Lane, J. Lukes, D. Bass, S.S. Bowser, M.W. Brown, F. Burki, M. Dunthorn, V. Hampl, A. Heiss, M. Hoppenrath, E. Lara, L. Le Gall, D.H. Lynn, H. McManus, E.A. Mitchell, S.E. Mozley-Stanridge, L.W. Parfrey, J. Pawlowski, S. Rueckert, L. Shadwick, C.L. Schoch, A. Smirnov, F.W. Spiegel, The revised classification of eukaryotes, J. Eukaryot. Microbiol. 59 (2012) 429–493.

[40] I.E. Gentle, A.J. Perry, F.H. Alcock, V.A. Likic, P. Dolezal, E.T. Ng, A.W. Purcell, M. McConnville, T. Naderer, A.L. Chanez, F. Charriere, C. Aschinger, A. Schneider, K. Tokatlidis, T. Lithgow, Conserved motifs reveal details of ancestry and structure in the small TIM chaperones of the mitochondrial intermembrane space, Mol. Biol. Evol. 24 (2007) 1149–1160.

[41] J.W. Allen, S.J. Ferguson, M.L. Ginger, Distinctive biochemistry in the trypanosome mitochondrial intermembrane space suggests a model for stepwise evolution of the MIA pathway for import of cysteine-rich proteins, FEBS Lett. 582 (2008) 2817–2825.

[42] E. Eckers, M. Cyrklaff, L. Simpson, M. Deponte, Mitochondrial protein import pathways are functionally conserved among eukaryotes despite compositional diversity of the import machineries, Biol. Chem. 393 (2012) 513–524.

[43] E. Eckers, C. Petrungaro, D. Gross, J. Riemer, K. Hell, M. Deponte, Divergent molecular evolution of the mitochondrial sulfhydryl: cytochrome C oxidoreductase Erv in opisthokonts and parasitic protists, J. Biol. Chem. 288 (2013) 2676–2688.

[44] S. Basu, J.C. Leonard, N. Desai, D.A. Mavridou, K.H. Tang, A.D. Goddard, M.L. Ginger, J. Lukes, J.W. Allen, Divergence of Erv1-associated mitochondrial import and export pathways in trypanosomes and anaerobic protists, Eukaryot. Cell 12 (2013) 343–355.

[45] C.D. Peikert, J. Mani, M. Morgenstern, S. Kaser, B. Knapp, C. Wenger, A. Harsman, S. Oeljeklaus, A. Schneider, B. Warscheid, Charting organellar importomes by quantitative mass spectrometry, Nat. Commun. 8 (2017) 15272.

[46] J.M. Kelly, H.M. Ward, M.A. Miles, G. Kendall, A shuttle vector which facilitates the expression of transfected genes in Trypanosoma cruzi and Leishmania, Nucleic Acids Res. 20 (1992) 3963–3969.

[47] A.F. Sousa, A.G. Gomes-Alves, D. Benitez, M.A. Comini, L. Flohe, T. Jaeger, J. Passos, F. Stuhlmann, A.M. Tomas, H. Castro, Genetic and chemical analyses reveal that trypanothione synthetase but not glutathionylspermidine synthetase is essential for Leishmania infantum, Free Radic. Biol. Med. 73 (2014) 229–238.

[48] A.V. Bryksin, I. Matsumura, Overlap extension PCR cloning: a simple and reliable way to create recombinant plasmids, BioTechniques 48 (2010) 463–465.

[49] V. Peleh, E. Cordat, J.M. Herrmann, Mia40 is a trans-site receptor that drives protein import into the mitochondrial intermembrane space by hydrophobic substrate binding, eLife (2016) 5.

[50] F. Sherman, Getting started with yeast, Methods Enzymol. 194 (1991) 3–21.

[51] D. Mumberg, R. Muller, M. Funk, Regulatable promoters of Saccharomyces cerevisiae: comparison of transcriptional activity and their use for heterologous expression, Nucleic Acids Res. 22 (1994) 5767–5768.

[52] R.D. Gietz, R.H. Schiestl, Quick and easy yeast transformation using the LiAc/SS carrier DNA/PEG method, Nat. Protoc. 2 (2007) 35–37.

[53] R.S. Sikorski, J.D. Boeke, *In vitro* mutagenesis and plasmid shuffling: from cloned gene to mutant yeast, Methods Enzymol. 194 (1991) 302–318.

[54] R.J. Simpson, Preparation of extracts from yeast, Cold Spring Harb. Protoc. (2011) (**2011**, pdb prot5545).

[55] S.B. Miller, C.T. Ho, J. Winkler, M. Khokhrina, A. Neuner, M.Y. Mohamed, D.L. Guilbride, K. Richter, M. Lisby, E. Schiebel, A. Mogk, B. Bukau, Compartment-specific aggregases direct distinct nuclear and cytoplasmic aggregate deposition, EMBO J. 34 (2015) 778–797.

[56] D. Mokranjac, S.A. Paschen, C. Kozany, H. Prokisch, S.C. Hoppins, F.E. Nargang, W. Neupert, K. Hell, Tim50, a novel component of the TIM23 preprotein translocase of mitochondria, EMBO J. 22 (2003) 816–825.

[57] M. Looke, K. Kristjuhan, A. Kristjuhan, Extraction of genomic DNA from yeasts for PCR-based applications, BioTechniques 50 (2011) 325–328.

[58] C.A. Sellick, R.N. Campbell, R.J. Reece, Galactose metabolism in yeast-structure and regulation of the leloir pathway enzymes and the genes encoding them, Int. Rev. Cell Mol. Biol. 269 (2008) 111–150.

[59] A. Chacinska, B. Guiard, J.M. Muller, A. Schulze-Specking, K. Gabriel, S. Kutik, N. Pfanner, Mitochondrial biogenesis, switching the sorting pathway of the intermembrane space receptor Mia40, J. Biol. Chem. 283 (2008) 29723–29729.

[60] D. Milenkovic, T. Ramming, J.M. Muller, L.S. Wenz, N. Gebert, A. Schulze-Specking, D. Stojanovski, S. Rospert, A. Chacinska, Identification of the signal directing Tim9 and Tim10 into the intermembrane space of mitochondria, Mol. Biol. Cell 20 (2009)

2530–2539.

[61] V. Peleh, J. Riemer, A. Dancis, J.M. Herrmann, Protein oxidation in the inter-membrane space of mitochondria is substrate-specific rather than general, Microb. Cell 1 (2014) 81–93.

[62] D.P. Sideris, N. Petrakis, N. Katrakili, D. Mikropoulou, A. Gallo, S. Ciofi-Baffoni, L. Banci, I. Bertini, K. Tokatlidis, A novel intermembrane space-targeting signal docks cysteines onto Mia40 during mitochondrial oxidative folding, J. Cell Biol. 187 (2009) 1007–1022.

[63] D.P. Sideris, K. Tokatlidis, Oxidative folding of small Tims is mediated by site-specific docking onto Mia40 in the mitochondrial intermembrane space, Mol. Microbiol. 65 (2007) 1360–1373.

[64] S. Romao, H. Castro, C. Sousa, S. Carvalho, A.M. Tomas, The cytosolic tryparedoxin of Leishmania infantum is essential for parasite survival, Int. J. Parasitol. 39 (2009) 703–711.

[65] A.C. Haindrich, M. Boudova, M. Vancova, P.P. Diaz, E. Horakova, J. Lukes, The intermembrane space protein Erv1 of Trypanosoma brucei is essential for mitochondrial Fe-S cluster assembly and operates alone, Mol. Biochem. Parasitol. 214 (2017) 47–51.

[66] T. Beneke, R. Madden, L. Makin, J. Valli, J. Sunter, E. Gluenz, A CRISPR Cas9 high-throughput genome editing toolkit for kinetoplastids, R. Soc. Open Sci. 4 (2017) 170095.

[67] L. Sollelis, M. Ghorbal, C.R. MacPherson, R.M. Martins, N. Kuk, L. Crobu, P. Bastien, A. Scherf, J.J. Lopez-Rubio, Y. Sterkers, First efficient CRISPR-Cas9-mediated genome editing in Leishmania parasites, Cell. Microbiol. 17 (2015) 1405–1412.

[68] W.W. Zhang, G. Matlashewski, CRISPR-Cas9-mediated genome editing in Leishmania donovani, mBio 6 (2015) e00861.

[69] G. Hofhaus, J.E. Lee, I. Tews, B. Rosenberg, T. Lisowsky, The N-terminal cysteine pair of yeast sulfhydryl oxidase Erv1p is essential for *in vivo* activity and interacts with the primary redox centre, Eur. J. Biochem. 270 (2003) 1528–1535.

[70] S.K. Ang, H. Lu, Deciphering structural and functional roles of individual disulfide bonds of the mitochondrial sulfhydryl oxidase Erv1p, J. Biol. Chem. 284 (2009)

28754–28761.

[71] S.K. Ang, M. Zhang, T. Lodi, H. Lu, Mitochondrial thiol oxidase Erv1: both shuttle cysteine residues are required for its function with distinct roles, Biochem. J. 460 (2014) 199–210.

[72] A. Levitan, A. Danon, T. Lisowsky, Unique features of plant mitochondrial sulfhy-dryl oxidase, J. Biol. Chem. 279 (2004) 20002–20008.

[73] E. Vitu, M. Bentzur, T. Lisowsky, C.A. Kaiser, D. Fass, Gain of function in an ERV/ALR sulfhydryl oxidase by molecular engineering of the shuttle disulfide, J. Mol. Biol. 362 (2006) 89–101.

[74] C.K. Wu, T.A. Dailey, H.A. Dailey, B.C. Wang, J.P. Rose, The crystal structure of augmenter of liver regeneration: a mammalian FAD-dependent sulfhydryl oxidase, Protein Sci.: Publ. Protein Soc. 12 (2003) 1109–1118.

[75] H. Lange, T. Lisowsky, J. Gerber, U. Muhlenhoff, G. Kispal, R. Lill, An essential function of the mitochondrial sulfhydryl oxidase Erv1p/ALR in the maturation of cytosolic Fe/S proteins, EMBO Rep. 2 (2001) 715–720.

[76] M.E. Sztolsztener, A. Brewinska, B. Guiard, A. Chacinska, Disulfide bond formation: sulfhydryl oxidase ALR controls mitochondrial biogenesis of human MIA40, Traffic 14 (2013) 309–320.

[77] V. Peleh, F. Zannini, S. Backes, N. Rouhier, J.M. Herrmann, Erv1 of Arabidopsis thaliana can directly oxidize mitochondrial intermembrane space proteins in the absence of redox-active Mia40, BMC Biol. 15 (2017) 106.

[78] P. Kritsiligkou, A. Chatzi, G. Charalampous, A. Mironov Jr., C.M. Grant, K. Tokatlidis, Unconventional targeting of a thiol peroxidase to the mitochondrial intermembrane space facilitates oxidative protein folding, Cell Rep. 18 (2017) 2729–2741.

[79] T.J. Tavender, J.J. Springate, N.J. Bulleid, Recycling of peroxiredoxin IV provides a novel pathway for disulphide formation in the endoplasmic reticulum, EMBO J. 29 (2010) 4185–4197.

[80] E. Zito, E.P. Melo, Y. Yang, A. Wahlander, T.A. Neubert, D. Ron, Oxidative protein folding by an endoplasmic reticulum-localized peroxiredoxin, Mol. Cell 40 (2010) 787–797.